Implications of an Electron-Hopping Model for Charge Transport through Donor−Bridge−Acceptor Assemblies Connected to Metal Electrodes

Norman Sutin,*,† Bruce S. Brunschwig,‡ Carol Creutz,† and Stephen W. Feldberg†

Chemistry Department, Brookhaven National Laboratory, Upton, New York 11973-5000, and Beckman Institute, California Institute of Technology, Mail Code 139-74, 1200 East California Boulevard, Pasadena, California 91125

Received: April 29, 2004; In Final Form: June 4, 2004

An electron-hopping model for electrode-to-electrode charge transport through donor-bridge-acceptor assemblies (*J. Phys. Chem. B* **2003**, *107*, 10687) is further developed by detailed electrostatic analysis of the assembly and treatment of the steady-state kinetics. Charge transport between the two electrodes proceeds via the D−B−A bridges: D transfers an electron to A through the bridge. The newly formed D^+ and A^- are then rapidly reduced and oxidized, respectively, at the electrodes giving rise to a steady state in which the current depends on the rate of electron transfer from D to A. The driving force dependence of the nuclear factor for the D to A electron transfer results in the current through the D−B−A bridge increasing with applied voltage (positive differential conductance) in the normal free-energy region but decreasing in the inverted region (negative differential conductance). The electronic factors can be manipulated by changing the separations between the electrodes and DBA or the length of B or by changing the nature of the bridge material. Decreasing the electronic factor for D to A electron transfer decreases the flux at a given applied voltage in the normal region, but the effect is much greater in the inverted region. Possible parallel tunneling and electron hopping mechanisms that could contribute to the current and interfere with the region of negative differential resistance are analyzed in detail. For the coupled electron-transfer sequence considered here, changing electronic factors result in dramatic shifts of the reaction profile.

1. Introduction

The behavior of molecules as conductors, swtiches, etc. is presently of great experimental and theoretical interest.[1−6] When a voltage is applied across a metal−molecule−metal assembly[7] electrons can tunnel across the bridge and, as the applied electric field brings the metal and bridging molecule orbital (LUMO or HOMO) levels to the same energy, resonant tunneling can occur.[8] In voltage regions far from resonance, a superexchange description of the tunneling includes the electronic energies of the bridge. However, the nuclear factors (λ, $\Delta G°$) that control the rate of electron transfer in solution[9] are absent from the description of the system's conductance.[10] In contrast, when the electron hops onto (and off) the bridge, the nuclear factors again become important.[11,12]

In an earlier paper, we discussed electron transfer between two metal electrodes joined by a donor−bridge−acceptor system.[11,13,14] We proposed that, when electron transfer occurs predominantly by a hopping mechanism, nuclear factors, along with the field resulting from the applied voltage, will control the current through the system. By utilizing D/A couples with small λ values (e.g., 0.5 eV), a region of negative differential resistance can be achieved at modest applied potentials. In this paper, we provide a detailed description of the kinetics of such a model system. In this model, neutral DA molecules isolated from one another connect two metal electrodes.[15−17] Charge transport between the two electrodes proceeds via the DA bridges via parallel paths 1a and 1b.

$$e^- + D^+A^- \rightleftharpoons DA^-$$
$$DA \rightleftharpoons D^+A^-$$
$$DA^- \rightleftharpoons DA + e^- \qquad \text{(Scheme 1a)}$$

and

$$e^- + D^+A \rightleftharpoons DA$$
$$DA \rightleftharpoons D^+A^-$$
$$D^+A^- \rightleftharpoons D^+A + e^- \qquad \text{(Scheme 1b)}$$

At steady state, the rates of both routes depend on the rate of electron transfer from D to A, $DA \rightarrow D^+A^-$. The key features of the system we will consider are as follows: The DA-bilayer contains no movable species. Electrons can move across the bilayer from one metal electrode to another only by hopping between an electrode and an adjacent redox moiety or by hopping from D to A; direct electronic tunneling between the electrodes or between an electrode and nonnearest redox species is excluded.

The remainder of the paper is divided into five sections. In section 2, we analyze the electrical and electrochemical potentials of the cell assembly. The chemical potential of the electron in the metal electrodes is a key factor and the dynamics of the system will depend critically upon the choice of the metals

* To whom correspondence should be addressed.
† Brookhaven National Laboratory.
‡ California Institute of Technology.

10.1021/jp048133k CCC: $27.50
Published on Web 07/16/2004

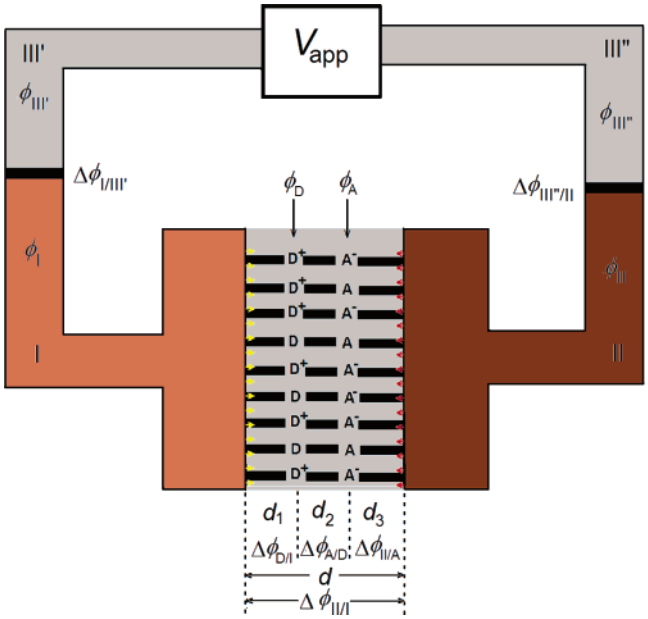

Figure 1. System schematic. Regions I, II, and III contain metals. D and A are separated from the electrodes (d_1, d_3) and from one another (d_2) by molecular bridging materials to be discussed later.[19] The region between I and II is denoted the DA bilayer.

and upon surface potentials. These are factors that have been shown to be important in organic LED systems.[18] In section 3, we examine the steady-state conditions and derive expressions for the concentrations of D^+A^-, DA, etc. in terms of the rate constants for the electrode and intramolecular electron transfer. In section 4, we provide semiclassical expressions for evaluation of the heterogeneous and intramolecular electron transfer rate constants. In section 5, we drastically limit the parameters of the system in order to produce a "simplified model" in which the response of the steady-state current to changing the applied field and the electronic and nuclear factors for electron transfer can be explored. In section 6, we give a detailed analysis of possible parallel tunneling and electron hopping mechanisms that could contribute to the current and interfere with the region of negative differential resistance.

2. Analysis of the Electrical and Electrochemical Potentials

There are two facets of this analysis: first we deduce the electrical potentials that effect electron transfer and second we consider the relevant chemical potentials. To simplify the analysis of the electrical potentials, we assume that the introduction of charge into the bilayer (by the oxidation or reduction of the redox moieties) does not significantly modify the electric field within the bilayer. In addition, we assume that the geometry is planar; that is, the electrodes are infinitely large and parallel so that edge effects are negligible and that the potential and electric fields are unaffected by the charges on D or A.

Analysis of the Electrical Potentials. The schematic for the system of interest is shown in Figure 1.

The different metals are identified as I, II, and III (III′ and III″ denote separate pieces of the same metal). Our objective is to deduce the potentials across and within the bilayer region separating metal phases I and II. Potentials ϕ_A and ϕ_D denote the electrical potentials at the loci of the A and D moieties. The potential V_{app} is the potential applied to the system. All potential differences denote the difference in the electrical potentials of the indicated phases (or locations within the phases) proceeding counterclockwise around the circuit. Thus (see Figure 1) $V_{app} = \phi_{III'} - \phi_{III''}$ and the differences in electrical potentials are $\Delta\phi_{I/III'} = \phi_I - \phi_{III'}$, $\Delta\phi_{II/I} = \phi_{II} - \phi_I$, $\Delta\phi_{D/I} = \phi_D - \phi_I$, $\Delta\phi_{A/D} = \phi_A - \phi_D$, $\Delta\phi_{II/A} = \phi_{II} - \phi_A$, $\Delta\phi_{D/I} = \phi_D - \phi_I$, and $\Delta\phi_{III/II} = \phi_{III} - \phi_{II}$. Moving an electron completely around the circuit requires no work so that

$$V_{app} + \Delta\phi_{I/III'} + \Delta\phi_{II/I} + \Delta\phi_{III''/II} = 0 \quad (1)$$

The yellow and red arrows are intended to denote the location but not the sign of the permanent surface dipoles with potentials S_I and S_{II}, respectively. The only potential difference term that can be controlled electrically is V_{app} but this will change $\Delta\phi_{II/I}$, the potential across the bilayer. We assume that the surface dipoles are located in a negligibly thin layer adjacent to the electrode surfaces; we use the same convention for the sign of the dipole as for all other potential differences. Then, with eq 1

$$\Delta\phi_{II/I} = -(V_{app} + \Delta\phi_{I/III'} + \Delta\phi_{III''/II}) = \frac{d\phi}{dx}d + S_I + S_{II} \quad (2)$$

where $d\phi/dx$ is the potential gradient within the bilayer. We can now deduce the electrical potential differences $\Delta\phi_{D/I}$, $\Delta\phi_{A/D}$, and $\Delta\phi_{II/A}$

$$\Delta\phi_{D/I} = d_1\frac{d\phi}{dx} + S_1 = -(\Delta\phi_{III''/II} + \Delta\phi_{I/III'} + V_{app} + S_I + S_{II})\frac{d_1}{d} + S_1 \quad (3)$$

$$\Delta\phi_{A/D} = -(\Delta\phi_{III''/II} + \Delta\phi_{I/III'} + V_{app} + S_I + S_{II})\frac{d_2}{d} \quad (4)$$

$$\Delta\phi_{II/A} = -(\Delta\phi_{III''/II} + \Delta\phi_{I/III'} + V_{app} + S_I + S_{II})\frac{d_3}{d} + S_{II} \quad (5)$$

The potential difference that will drive the electron-transfer reactions, $e^- + D^+A^- \rightleftharpoons DA^-$ and $e^- + D^+A \rightleftharpoons DA$, at electrode I is $\phi_D - \phi_{III'}$

$$\phi_D - \phi_{III'} = \Delta\phi_{I/III'} + \Delta\phi_{D/I} = \Delta\phi_{I/III'} - (\Delta\phi_{III''/II} + \Delta\phi_{I/III'} + V_{app} + S_I + S_{II})\frac{d_1}{d} + S_I \quad (6)$$

Similarly, the potential difference that will drive the electron-transfer reactions, $D^+A^- \rightleftharpoons e^- + D^+A$ and $DA^- \rightleftharpoons e^- + DA$, at electrode II is $\phi_{III''} - \phi_A$

$$\phi_{III''} - \phi_A = \Delta\phi_{III''/II} + \Delta\phi_{II/A} = \Delta\phi_{III''/II} - (\Delta\phi_{III''/II} + \Delta\phi_{I/III'} + V_{app} + S_I + S_{II})\frac{d_3}{d} + S_{II} \quad (7)$$

It is apparent from the above equations that when $d_1/d \rightarrow 0$ and $d_3/d \rightarrow 0$ the dependence of the interfacial electron transfer on V_{app} is virtually eliminated (see eqs 6 and 7). Then, the only ways to alter $(\phi_D - \phi_{III'})$ or $(\phi_A - \phi_{III''})$ are to use different metals for the electrodes, thereby modifying the values of $\Delta\phi_{I/III'}$ and $\Delta\phi_{III''/II}$ and/or chemically modify the interface to change the values of S_I and S_{II}.

Chemical Potential Differences. In addition to the electrical potential differences, the electron-transfer reactions are also driven by chemical potential differences. Since metals III′ and III″ are identical their chemical potentials are the same, i.e., $\mu_{III'} = \mu_{III''} = \mu_{III}$. Thus, the differences between the standard chemical potential of an electron in metal III′ and in the D^+/D redox couple and between the A/A^- redox couple and metal III″ are, respectively

$$\mu^0_{D^+/D} - \mu_{III} = -(eE^0_{D^+/D} + \mu_{III}) \quad (8)$$

$$\mu_{III} - \mu^0_{A/A^-} = \mu_{III} + eE^0_{A/A^-} \quad (9)$$

where

$$\mu^0_{D^+/D} = (\mu^0_D - \mu^0_{D^+}) \quad (10)$$

$$\mu^0_{A/A^-} = (\mu^0_{A^-} - \mu^0_A) \quad (11)$$

and

$$\mu^0_{A/A^-} - \mu^0_{D^+/D} = -e(E^0_{A/A^-} - E^0_{D^+/D}) \quad (12)$$

The value of $E^0_{D^+/D}$, the standard potential of the D^+/D couple, is assumed independent of the oxidation state of DA, as is E^0_{A/A^-}, the standard potential of the A/A^- couple. The electrochemical and redox potentials must be expressed on the same scale, for example the vacuum scale for which the potential of the normal hydrogen electrode is $\sim+(4.4-4.5)$ V.[20] Note that the sign of the potential used here is consistent with electrochemical notation.

Standard Electrochemical Free-Energy Changes. The standard free-energy changes for the electrode reactions are obtained by adding the electrical and chemical free-energy changes. Thus for the reduction of D^+ at electrode I

$$\Delta\bar{G}^0_1 = -e(\phi_D - \phi_{III'}) + (\mu^0_{D^+/D} - \mu_{III}) \quad (13)$$

Substitution from eqs 6 and 8 gives

$$\Delta\bar{G}^0_1 = e\left[(\Delta\phi_{III''/II} + \Delta\phi_{I/III'} + V_{app} + S_I + S_{II})\frac{d_1}{d} - S_I - \Delta\phi_{I/III'}\right] - \mu_{III} - eE^0_{D^+/D} \quad (14)$$

Provided that the electrochemical potentials of metals I and III′ are the same and also those of II and III″

$$\Delta\bar{G}^0_1 = -e\left[\left(\frac{\mu_I - \mu_{II}}{e} + V_{app} + S_I + S_{II}\right)\frac{d_1}{d} - S_I\right] - \mu_I - eE^0_{D^+/D} = e(E_1 - E^0_{D^+/D}) \quad (15)$$

where

$$E_1 = \left(\frac{\mu_I - \mu_{II}}{e} + V_{app} + S_I + S_{II}\right)\frac{d_1}{d} - S_I - \frac{\mu_I}{e} \quad (16)$$

Similarly for the oxidation of A^- at electrode II

$$\Delta\bar{G}^0_3 = -e(\phi_{III''} - \phi_A) + (\mu_{III} - \mu^0_{A/A^-}) \quad (17)$$

Substitution from eqs 7 and 9 gives

$$\Delta\bar{G}^0_3 = e\left[(\Delta\phi_{III''/II} + \Delta\phi_{I/III'} + V_{app} + S_I + S_{II})\frac{d_3}{d} - S_{II} - \Delta\phi_{III''/II}\right] + \mu_{III} + eE^0_{A/A^-} \quad (18)$$

Again assuming that the electrochemical potentials of metals I and III′ and also those of II and III″ are the same

$$\Delta\bar{G}^0_3 = e\left[\left(\frac{\mu_I - \mu_{II}}{e} + V_{app} + S_I + S_{II}\right)\frac{d_3}{d} - S_{II}\right] + \mu_{II} + eE^0_{A/A^-} = -e(E_3 - E^0_{A/A^-}) \quad (19)$$

where

$$E_3 = -\left(\frac{\mu_I - \mu_{II}}{e} + V_{app} + S_I + S_{II}\right)\frac{d_3}{d} + S_{II} - \frac{\mu_{II}}{e} \quad (20)$$

The standard electrochemical free-energy change for the D to A electron transfer is similarly given by the sum of the electrical and chemical free-energy changes

$$\Delta\bar{G}^0_2 = -e(\phi_A - \phi_D) + \mu^0_{A/A^-} - \mu^0_{D^+/D} \quad (21)$$

Substituting for $(\phi_A - \phi_D) = \Delta\phi_{A/D}$ from eq 4, for $(\mu^0_{A/A^-} - \mu^0_{D^+/D})$ from eq 10 and making the same assumption about the metal electrochemical potentials as above gives

$$\Delta\bar{G}^0_2 = e\left[\left(\frac{\mu_I - \mu_{II}}{e} + V_{app} + S_I + S_{II}\right)\frac{d_2}{d} - (E^0_{A/A^-} - E^0_{D^+/D})\right] \quad (22)$$

Summing eqs 11, 16 and 21, it readily follows that[21]

$$\Delta\bar{G}^0_1 + \Delta\bar{G}^0_2 + \Delta\bar{G}^0_3 = eV_{app} \quad (23)$$

As noted earlier, the potentials E_1, E_3, $E^0_{D^+/D}$, E^0_{A/A^-}, etc. must be expressed on the same scale, for example the vacuum scale for which the potential of the normal hydrogen electrode is $\sim+(4.4-4.5)$ V.[20] Note also that the driving forces and electrode potentials are independent of the nature of metal III.

3. Steady-State Relations

We assume that the metal electrodes are large and parallel and that the donor−acceptor pair comprises a *dilute* layer of molecular bridges joining metals I and II: [metal I]−D−A−[metal II] (see Figure 1). With the concentrations of each state denoted by Γ_{DA}, $\Gamma_{D^+A^-}$, Γ_{D^+A}, and Γ_{DA^-}, by *dilute* we mean that the total concentration of all the bridges, Γ_{total} ($=\Gamma_{DA} + \Gamma_{D^+A^-} + \Gamma_{D^+A} + \Gamma_{DA^-}$) is considerably less than a monolayer. There are four possible states of any given [metal I]−D−A−[metal II] assembly: [metal I]−D−A−[metal II], [metal I]−D^+−A^-−[metal II], [metal I]−D^+−A−[metal II], and [metal I]−D−A^-−[metal II].

Redox moiety D (or D^+) is at distance d_1 from the surface of metal I; redox moiety A (or A^-) is at distance d_3 from the surface of metal II. The distance between D (or D^+) and A (or A^-) is d_2 (see Figure 1). We are concerned with three specific electron-transfer reactions: an intramolecular electron-transfer reaction and two heterogeneous electron-transfer reactions.

The intramolecular electron transfer is represented by

$$DA \underset{k_{-2}}{\overset{k_2}{\rightleftharpoons}} D^+A^- \tag{24}$$

where k_2 and k_{-2} (units of s^{-1}) are the forward and reverse rate constants.[22] The heterogeneous electron-transfer reactions occurring at metal I are

$$e^-(I) + D^+A \underset{k_{-1}}{\overset{k_1}{\rightleftharpoons}} DA \tag{25}$$

and

$$e^-(I) + D^+A^- \underset{k_{-1}}{\overset{k_1}{\rightleftharpoons}} DA^- \tag{26}$$

The thermodynamics and kinetics of eqs 25 and 26 are assumed to be identical.[23] Thus, the forward and reverse reaction rates will be $k_1(\Gamma_{D^+A} + \Gamma_{D^+A^-})$ and $k_{-1}(\Gamma_{DA} + \Gamma_{DA^-})$. We also assume that reactions 25 and 26 cannot occur at metal II.

In contrast to electrode I, at electrode II, it is oxidation by the electrode that carries the process. The analogous electron-transfer reactions occurring at metal II (which cannot occur at metal I) are

$$DA^- \underset{k_{-3}}{\overset{k_3}{\rightleftharpoons}} DA + e^-(II) \tag{27}$$

$$D^+A^- \underset{k_{-3}}{\overset{k_3}{\rightleftharpoons}} D^+A + e^-(II) \tag{28}$$

The thermodynamics and kinetics of these reactions are also assumed to be identical. The forward (left to right) and reverse reaction rates will be $k_3(\Gamma_{DA^-} + \Gamma_{D^+A^-})$ and $k_{-3}(\Gamma_{DA} + \Gamma_{D^+A})$.

The four linear equations for the steady-state condition are the mass balance equation

$$\Gamma_{total} = \Gamma_{D^+A^-} + \Gamma_{D^+A} + \Gamma_{DA^-} + \Gamma_{DA} \tag{29}$$

and the following three steady-state expressions:

$$\frac{d\Gamma_{DA^-}}{dt} = 0 = k_{-3}\Gamma_{DA} + k_1\Gamma_{D^+A^-} - (k_{-1} + k_3)\Gamma_{DA^-} \tag{30}$$

$$\frac{d\Gamma_{D^+A}}{dt} = 0 = k_{-1}\Gamma_{DA} + k_3\Gamma_{D^+A^-} - (k_1 + k_{-3})\Gamma_{D^+A} \tag{31}$$

$$\frac{d\Gamma_{DA}}{dt} = 0 = k_{-2}\Gamma_{D^+A^-} + k_1\Gamma_{D^+A} + k_3\Gamma_{DA^-} - (k_{-1} + k_2 + k_{-3})\Gamma_{DA} \tag{32}$$

The individual concentrations deduced from them are then

$$\Gamma_{DA} = \Gamma_{total}\frac{N(k_1 + k_{-3})(k_{-1} + k_3)}{MR + NS} \tag{33}$$

$$\Gamma_{D^+A^-} = \Gamma_{total}\frac{M(k_1 + k_{-3})(k_{-1} + k_3)}{MR + NS} \tag{34}$$

$$\Gamma_{D^+A} = \Gamma_{total}\frac{(k_{-1} + k_3)(k_{-1}N + k_3M)}{MR + NS} \tag{35}$$

$$\Gamma_{DA^-} = \Gamma_{total}\frac{(k_1 + k_{-3})(k_1M + k_{-3}N)}{MR + NS} \tag{36}$$

and the steady-state electron flux, f_e, is

$$f_e = k_2\Gamma_{DA} - k_{-2}\Gamma_{D^+A^-} = \Gamma_{total}\frac{(k_1 + k_{-3})(k_{-1} + k_3)(k_2N - k_{-2}M)}{MR + NS} \tag{37}$$

where

$$M = k_{-1}k_{-3}(k_{-1} + k_3) + (k_{-1}k_2 + k_2k_3 + k_{-1}k_{-3})(k_1 + k_{-3}) \tag{38}$$

$$N = k_1k_3(k_{-1} + k_3) + (k_1k_3 + k_{-1}k_{-2} + k_{-2}k_3)(k_1 + k_{-3}) \tag{39}$$

$$R = k_3(k_{-1} + k_3) + (k_1 + k_{-3})(k_1 + k_{-1} + k_3) \tag{40}$$

$$S = k_{-1}(k_{-1} + k_3) + (k_1 + k_{-3})(k_{-1} + k_3 + k_{-3}) \tag{41}$$

$$k_2N - k_{-2}M = (k_1 + k_{-1} + k_3 + k_{-3})(k_1k_2k_3 - k_{-1}k_{-2}k_{-3}) \tag{42}$$

4. Evaluation of the Electrode and Intramolecular Rate Constants

Intramolecular Reaction. The forward and reverse rate constants (k_2, k_{-2}) for the intramolecular electron-transfer step (eq 24) are obtained from the products $k_2 = A_2\kappa_{n,2}$ and $k_{-2} = A_2\kappa_{n,-2}$, respectively, where A_2, the electronic factor (s^{-1}), and the nuclear factors, $\kappa_{n,2}$ and $\kappa_{n,-2}$, are given by[9]

$$A_2 = \frac{2\pi^{3/2}(H_2^0)^2}{h(\lambda_2 k_B T)^{1/2}}\exp[-\beta_2(d_2 - d_2^0)] \tag{43}$$

$$\kappa_{n,2} = \exp\left[-\frac{(\lambda_2 - e[\Delta\phi_{A/D} + E^0_{A/A^-} - E^0_{D^+/D}])^2}{4\lambda_2 k_B T}\right] \tag{44}$$

$$\kappa_{n,-2} = \exp\left[-\frac{(\lambda_2 + e[\Delta\phi_{A/D} + E^0_{A/A^-} - E^0_{D^+/D}])^2}{4\lambda_2 k_B T}\right] \tag{45}$$

In the above expressions, H_2^0 is the donor−acceptor electronic coupling element at separation d_2^0, β_2 characterizes the distance dependence of the coupling element, and λ_2 is the reorganization energy. The driving forces for the forward and reverse reactions are $-e(\Delta\phi_{A/D} + E^0_{A/A^-} - E^0_{D^+/D})$ and $+e(\Delta\phi_{A/D} + E^0_{A/A^-} - E^0_{D^+/D})$, respectively.

Note that at equilibrium

$$\frac{k_2}{k_{-2}} = K_2 = \frac{\Gamma_{D^+A^-}}{\Gamma_{DA}} = \exp\left[\frac{e}{k_B T}(\Delta\phi_{A/D} + E^0_{A/A^-} - E^0_{D^+/D})\right] \tag{46}$$

and that $k_2 = k_{-2} = k_2^0$ when $\Delta\phi_{A/D} + E^0_{A/A^-} - E^0_{D^+/D} = 0$ where

$$k_2^0 = \frac{2\pi^{3/2}(H_2^0)^2}{h\sqrt{\lambda_2 k_B T}}\exp[-\beta_2(d_2 - d_2^0)]\exp\left[-\frac{\lambda_2}{4k_B T}\right] \tag{47}$$

On the other hand, the reaction is barrierless and k_2 reaches its maximum value, $k_{2,max} = A_2$, when $\Delta\phi_{A/D} + E^0_{A/A^-} = -\lambda_2$.

Electrode Reactions. The forward and reverse reaction rates at electrode I (eqs 25, 26) are $k_1(\Gamma_{D^+A} + \Gamma_{D^+A^-})$ and $k_{-1}(\Gamma_{DA} + \Gamma_{DA^-})$. The rate constants, k_1 and k_{-1}, are a function of the driving force, $+e(E_1 - E^0_{D^+/D})$ and $-e(E_1 - E^0_{D^+/D})$, respectively, and the reorganization energy, λ_1, and are obtained from

the products $A_1\kappa_{n,1}$ and $A_1\kappa_{n,-1}$ where the electronic factor A_1 (s^{-1}) and the nuclear factors $\kappa_{n,1}$ and $\kappa_{n,-1}$ are given by[24-26]

$$A_1 = \frac{2\pi^{5/2}\rho_I(H_1^0)^2}{h}\left(\frac{k_BT}{\lambda_1}\right)^{1/2}\exp[-\beta_1(d_1 - d_1^0)] \quad (48)$$

$$\kappa_{n,1} = \exp\left[-\frac{(\lambda_1 + 2e(E_1 - E^0_{D^+/D}))}{4k_BT}\right] \times \int_{-\infty}^{\infty}\frac{\exp\left[\frac{-(\epsilon - e(E_1 - E^0_{D^+/D}))^2}{4\lambda_1 k_BT}\right]}{2\cosh\left[\frac{\epsilon}{2k_BT}\right]}\frac{d\epsilon}{k_BT} \quad (49)$$

$$\kappa_{n,-1} = \exp\left[-\frac{(\lambda_1 - 2e(E_1 - E^0_{D^+/D}))}{4k_BT}\right] \times \int_{-\infty}^{\infty}\frac{\exp\left[\frac{-(\epsilon - e(E_1 - E^0_{D^+/D}))^2}{4\lambda_1 k_BT}\right]}{2\cosh\left[\frac{\epsilon}{2k_BT}\right]}\frac{d\epsilon}{k_BT} \quad (50)$$

where ρ_I is the density of states (eV^{-1}) in metal electrode I, H_1^0 is the electrode I-donor electronic coupling element at separation d_1^0, and ϵ is the difference between the energy of the transferring electron and its electrochemical potential (Fermi energy) in electrode I (the latter is assumed equal to its electrochemical potential in metal III′).

Note that at equilibrium

$$\frac{k_1}{k_{-1}} = \frac{\Gamma_{DA} + \Gamma_{DA^-}}{\Gamma_{D^+A} + \Gamma_{D^+A^-}} = K_1 = \exp\left[-\frac{e}{k_BT}(E_1 - E^0_{D^+/D})\right] \quad (51)$$

and that, $k_1 = k_{-1} = k_1^0$ when $E_1 - E^0_{D^+/D} = 0$ where k_1^0 is defined as

$$k_1^0 = \frac{2\pi^{5/2}\rho_I(H_I^0)^2}{h}\sqrt{\frac{k_BT}{\lambda_1}}\exp[-\beta_1(d_1 - d_1^0)]\exp\left[-\frac{\lambda_1}{4k_BT}\right] \times \int_{-\infty}^{\infty}\frac{\exp\left[-\frac{\epsilon^2}{4\lambda_1 k_BT}\right]}{2\cosh\left[\frac{\epsilon}{2k_BT}\right]}\frac{d\epsilon}{k_BT} \quad (52)$$

On the other hand, the reaction is barrierless and k_1 reaches its limiting value

$$k_{1,lim} = A_1(4\lambda_1/\pi k_BT)^{1/2} \quad (53)$$

when $e(E_1 - E^0_{D^+/D}) = -2\lambda_1$.[27,28]

The expressions for the electrode reactions at metal II (k_3 and k_{-3}, eqs 27 and 28) are analogous to those given above. The forward and reverse reaction rates are $k_3(\Gamma_{DA^-} + \Gamma_{D^+A^-})$ and $k_{-3}(\Gamma_{DA} + \Gamma_{D^+A})$. The rate constants k_3 and k_{-3}, with driving forces, $-(E_3 - E^0_{A/A^-})$ and $+(E_3 - E^0_{A/A^-})$, respectively and reorganization energy, λ_3, are obtained from the products $A_3\kappa_{n,3}$ and $A_3\kappa_{n,-3}$, where the electronic factor A_3 (s^{-1}) and the nuclear factors $\kappa_{n,3}$ and $\kappa_{n,-3}$ are

$$A_3 = \frac{2\pi^{5/2}\rho_{II}(H_3^0)^2}{h}\left(\frac{k_BT}{\lambda_3}\right)^{1/2}\exp[-\beta_3(d_3 - d_3^0)] \quad (54)$$

$$\kappa_{n,3} = \exp\left[-\frac{(\lambda_1 - 2e(E_3 - E^0_{A/A^-}))}{4k_BT}\right] \times \int_{-\infty}^{\infty}\frac{\exp\left[\frac{-(\epsilon - e(E_3 - E^0_{A/A^-}))^2}{4\lambda_3 k_BT}\right]}{2\cosh\left[\frac{\epsilon}{2k_BT}\right]}\frac{d\epsilon}{k_BT} \quad (55)$$

$$\kappa_{n,-3} = \exp\left[-\frac{(\lambda_1 + 2e(E_3 - E^0_{A/A^-}))}{4k_BT}\right] \times \int_{-\infty}^{\infty}\frac{\exp\left[\frac{-(\epsilon - e(E_3 - E^0_{A/A^-}))^2}{4\lambda_3 k_BT}\right]}{2\cosh\left[\frac{\epsilon}{2k_BT}\right]}\frac{d\epsilon}{k_BT} \quad (56)$$

where ρ_{II} is the density of states (eV^{-1}) in metal electrode II, H_3^0 is the acceptor-electrode II electronic coupling element at separation d_3^0, and ϵ is the difference between the energy of the transferring electron and its electrochemical potential (Fermi energy) in electrode II (the latter is assumed the same as its electrochemical potential in metal III″).

Note that at equilibrium

$$\frac{k_3}{k_{-3}} = \frac{\Gamma_{D+A} + \Gamma_{DA}}{\Gamma_{D+A^-} + \Gamma_{DA^-}} = K_3 = \exp\left[\frac{e}{k_BT}(E_3 - E^0_{A/A^-})\right] \quad (57)$$

and that $k_3 = k_{-3} = k_3^0$ when $E_3 - E^0_{A/A^-} = 0$, where k_3^0 is defined as

$$k_3^0 = \frac{2\pi^{5/2}\rho_{II}(H_{II}^0)^2}{h}\sqrt{\frac{k_BT}{\lambda_3}}\exp[-\beta_3(d_3 - d_3^0)]\exp\left[-\frac{\lambda_3}{4k_BT}\right] \times \int_{-\infty}^{\infty}\frac{\exp\left[-\frac{\epsilon^2}{4\lambda_3 k_BT}\right]}{2\cosh\left[\frac{\epsilon}{2k_BT}\right]}\frac{d\epsilon}{k_BT} \quad (58)$$

On the other hand, the reaction is barrierless and k_1 reaches its limiting value

$$k_{3,lim} = A_3(4\lambda_3/\pi k_BT)^{1/2} \quad (59)$$

when $e(E_3 - E^0_{A/A^-}) = -2\lambda_3$.[27,28]

Note the nontraditional relationship here, i.e., k_3, the rate constant for the "forward" reaction, is an oxidation and k_{-3}, the rate constant for the "backward" reaction is a reduction.

5. A Simplified Model

The above analysis has shown that the rates of the intramolecular and electrode reactions depend on a number of parameters including the standard reduction potentials of the donor and acceptor couples, the applied voltage, the distance separating the redox sites, the chemical potentials of the metals, and the

electrostatic potentials of surface dipoles. To illustrate the principal features of the kinetics, (1) we assume that DBA is symmetrically located between the electrodes, (2) we ignore any surface dipole potentials, and (3) we assume that metals I and II are identical.

We further assume that (1) the chemical potential of the metal selected is equal to the average of the standard chemical potentials of the donor and acceptor couples and that (2) the interaction of the terminal bridging groups with the electrodes is sufficiently weak that the molecular system is not perturbed by binding to the electrodes.

These assumptions lead to a considerable simplification of the expressions for the driving forces for the reactions

$$\mu_I = \mu_{II} = (\mu^0_{A/A^-} + \mu^0_{D^+/D})/2 = -e(E^0_{A/A^-} + E^0_{D^+/D})/2 \quad (60)$$

As a consequence the driving forces for the electrode reactions are equal and are given by[11,20]

$$\Delta\bar{G}^0_1 = \Delta\bar{G}^0_3 = e[(E^0_{A/A^-} - E^0_{D^+/D})/2 + (d - d_2)V_{app}/2d] \quad (61)$$

whereas the driving force for the intramolecular electron transfer is[11,20]

$$\Delta\bar{G}^0_2 = -e[(E^0_{A/A^-} - E^0_{D^+/D}) - d_2V_{app}/d] \quad (62)$$

Further, if the donor and acceptor couples have identical reorganization energies and their coupling elements to the electrodes are the same, then $k_1 = k_3$ and $k_{-1} = k_{-3}$. In this circumstance, the steady-state concentrations of the individual species are given by

$$\Gamma_{DA} = \Gamma_{total}\frac{Q(1 + K_1)}{P(1 + 3K_1) + Q(3 + K_1)} \quad (63)$$

$$\Gamma_{D^+A^-} = \Gamma_{total}\frac{P(1 + K_1)}{P(1 + 3K_1) + Q(3 + K_1)} \quad (64)$$

$$\Gamma_{D^+A} = \Gamma_{DA^-} = \Gamma_{total}\frac{(PK_1 + Q)}{P(1 + 3K_1) + Q(3 + K_1)} \quad (65)$$

and the steady-state electron flux is

$$f_e = k_2\Gamma_{DA} - k_{-2}\Gamma_{D^+A^-} = \Gamma_{total}\frac{(1 + K_1)}{P(1 + 3K_1) + Q(3 + K_1)}(k_2Q - k_{-2}P) \quad (66)$$

where

$$K_1 = K_3 = k_1/k_{-1} = k_3/k_{-3} \quad (67)$$

$$P = k_2(k_1 + k_{-1}) + 2k_{-1}^2 \quad (68)$$

$$Q = k_{-2}(k_1 + k_{-1}) + 2k_1^2 \quad (69)$$

$$k_2Q - k_{-2}P = 2(k_1^2k_2 - k_{-1}^2k_{-2}) \quad (70)$$

Note that $\Gamma_{DA} \rightarrow \Gamma_{total}$ and $f_e \rightarrow k_2\Gamma_{total}$ when K_1, $K_2 \gg 1$ and $k_1 \gg k_2$. Under these conditions, the electrode reactions are Nernstian.

We next explore the behavior of the rate constants and electron fluxes for the simplified model. The electron fluxes are determined by the rate constants for the coupled electron-transfer reactions and by the concentrations of the intermediates. The individual rate constants are the products of nuclear and electronic factors, which can, to some extent, be controlled independently. The nuclear factors are determined by driving force and reorganization terms. Variation of the bridge length can be used to change the thermodynamics of the different electron-transfer steps and, accordingly, their nuclear factors. Manipulation of the bridges also provides one tool for enhancing the rate of the electrode reactions over the intramolecular process by manipulating the electronic factors. The electronic factors are sensitive to both bridge length and the nature of the bridging material.

Nuclear Factors. The above assumptions simplify the calculation of the nuclear factors. As pointed out earlier, when the driving force for the electrode reactions is increased, k_1 and k_3 reach limiting values of $k_{1,(3)lim} = A_{1,(3)}(4\lambda_{1,(3)}/\pi k_BT)^{1/2}$, respectively, when $\Delta\bar{G}^0_{1,(3)} = -(+)2\lambda_{1,(3)}$. When the reorganization of the medium can be neglected (or $d_1 = d_3 \simeq d_2/2$), the reorganization energy for the electrode reactions will be approximately half that for the intramolecular electron-transfer reaction, i.e., $\lambda_1 = \lambda_3 \simeq \lambda_2/2$.[27,28] Under these conditions, the V_{app} needed to achieve the limiting rate is

$$-eV_{app} = \frac{d}{d - d_2}[2\lambda_2 + e\Delta E^0] \quad (71)$$

where $\Delta E^0 = E^0_{A/A^-} - E^0_{D^+/D}$. Similarly, when the driving force for the intramolecular electron transfer is increased, k_2 reaches its maximum value of A_2 when $-\Delta\bar{G}^0_2 = \lambda_2$ or

$$-eV_{app} = \frac{d}{d_2}[\lambda_2 - e\Delta E^0] \quad (72)$$

Note that ΔE^0 shifts the V_{app} needed to reach the limiting electrochemical and maximum intramolecular rate constants in opposite directions. Moreover, it is apparent from eqs 61 and 62 that when $\Delta E^0 = 0$ and $d_1 = d_2 = d_3$, the driving forces for the electrode and intramolecular electron transfers will be the same and equal to $-eV_{app}/3$. Under these conditions, the reactions will be in phase and their rates will increase with driving force as long as $-eV_{app} \leq 2\lambda_1 = 2\lambda_3 = \lambda_2$. When $-eV_{app} = 2\lambda_1 = 2\lambda_3 = \lambda_2$, the rate constants for the electrode reactions will reach their limiting values, and the rate constant for the intramolecular electron-transfer rate will have its maximum value.

Earlier,[11] the variation of the nuclear factor with V_{app} was explored extensively. Figure 2a,b illustrates points we wish to emphasize here. First, as discussed above, the electrode rate constants do not become inverted but rather level off at a limiting value, in contrast to the rate constants for the intramolecular electron transfer. Second, the nuclear factor can be changed by variation of the separation distances d_1, d_2, and d_3 at constant d. Thus, consistent with eq 72, the onset of the inverted region is offset by 0.5 V in Figure 2b ($d/d_2 = 3$) compared to Figure 2a ($d/d_2 = 2$), although both use the same electronic factors (10^{11} s^{-1}) and reorganization energies ($\lambda_2 = 0.5$ eV, $\lambda_{1,3} = 0.25$ eV). Further, in contrast to Figure 2a, the electrode and intramolecular rate constants are in phase (limiting or maximizing at the same V_{app}) in Figure 2b where $d_1 = d_3 = d_2$. The relationship between $\log(k_2)$ and $\log(f_e)$ (which are very similar here) is discussed in "Concentration and Free-Energy Profiles" below.

Electronic Factors. Experimental work has amply demonstrated how significantly the nature of a bridging material can affect the electronic factor.[10,29] Thus, the limiting electronic

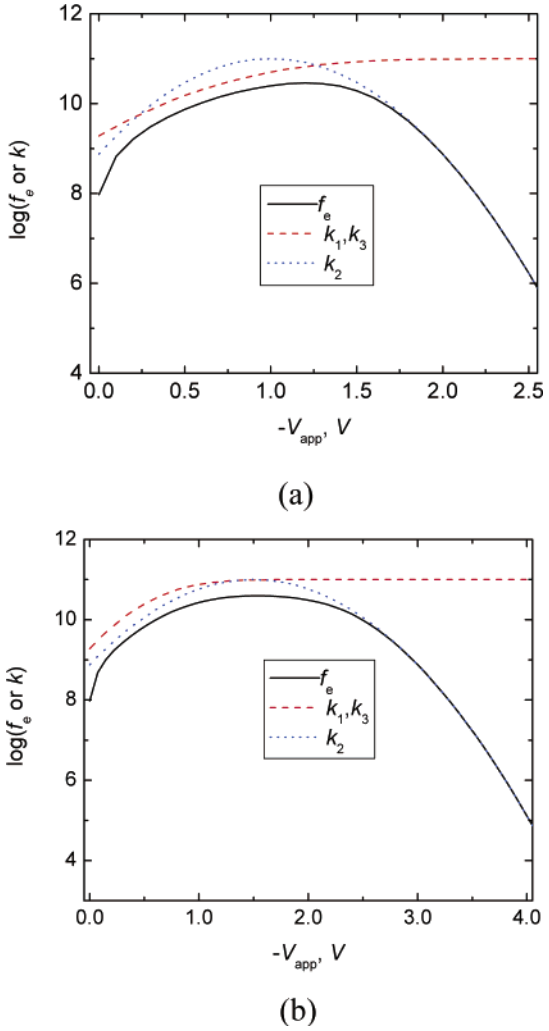

Figure 2. Electron flux (solid black), electrode rate constants (dashed red), and intramolecular (dotted green) electron-transfer rate constants as a function of applied voltage with electronic factors $A_{1,3} = A_2 = 10^{11}$ s^{-1} and $\lambda_2 = 0.5$ eV, $\lambda_{1,3} = 0.25$ eV for separation distances: (a) (left), $d_1 = d_3 = d_2/2$, and (b) (right), $d_1 = d_3 = d_2$. $\Delta E^\circ = E^0_{A/A^-} - E^0_{D^+/D} = 0$.

factors for ferrocene to gold (electrode) electron-transfer range from 10^{11} s^{-1} to 5×10^9 s^{-1} for oligo(phenylene vinylene) and alkane bridges, respectively, and these factors are attenuated exponentially by 0.5 and 1.1 per Å, respectively, as the bridge length is increased.[30] Mediation of electron transfer by a bridging group is conveniently considered in terms of a superexchange formalism in which orbitals of the bridge are mixed with those of the donor and acceptor. For a symmetrical system in which the bridge consists of n identical units, the donor−acceptor electronic coupling element H_{if} is given by[31]

$$H_{if} = \frac{T^2}{\Delta}\left(\frac{t}{\Delta}\right)^{n-1} \tag{73}$$

where T is the matrix element coupling the donor and acceptor orbitals, Δ is the difference between the energy of the bridge units and the energy of the donor and acceptor sites, t is the matrix element coupling adjacent bridge units, and $n \geq 1$. The donor−acceptor coupling decreases with distance

$$H_{if} = H^0_{if} \exp[-\beta(d - d^0)/2] \tag{74}$$

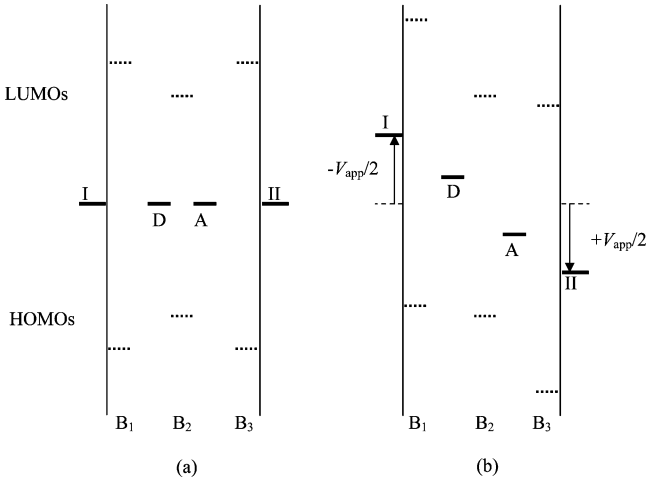

Figure 3. Shift in energy levels in the absence (a) and presence (b) of an applied field.

and, in terms of this model

$$\beta = \frac{2}{l}\ln\left(\frac{\Delta}{t}\right) \tag{75}$$

where l is the length of a bridge subunit ($l = (d - d^0)/(n - 1)$). The exponential distance dependence of the coupling element applies only to homogeneous bridging systems and has been incorporated, for example, in eqs 43, 48, and 54. More generally, the donor−acceptor coupling element is

$$H_{if} = \frac{T_{i,1}T_{n,f}}{\Delta_1}\Pi_{j=1}^{n-1}\left(\frac{t_{j,j+1}}{\Delta_{j+1}}\right) \tag{76}$$

Thus, for a given separation, the coupling interaction can be decreased by increasing the energy gaps and/or by decreasing t_j through the judicious exploitation of stereoelectronic effects.[29] In the simplified model being explored here, the energies of the sites are degenerate in the absence of an applied voltage (Figure 3a).

The superexchange coupling of I and II may involve the LUMOs of the bridging groups (electron transfer), the HOMOs (hole transfer), or both. If the energies of the sites are midway between the HOMOs and LUMOs, then the Δ_j will be the same for electron and hole transfer pathways and the dominant superexchange path will be determined by the transfer integrals. The degeneracy of the sites will be removed when a voltage is applied (Figure 3b). As I is made more negative and II more positive, the filled electronic levels of I move closer to the LUMO of B_1 and the levels of II move closer to the HOMO of B_3, decreasing the corresponding energy gaps. These energy-gap shifts will serve to increase the electronic factors for the electrode reactions relative to those for the intramolecular electron transfer. The difference between the electronic factors for the reactions can be further increased through the use of unsaturated bridges ($\beta \sim 0.2$ Å^{-1}) for the electrode reactions and saturated bridges ($\beta \sim 0.6$−1.0 Å^{-1}) for the intramolecular process (or vice versa). Controlling the electronic factors by suitable choice of bridging materials rather than by changing the separation distance has the advantage of keeping the nuclear factors constant.

Concentration and Free-Energy Profiles. The steady-state concentrations and the net electron flux are plotted vs V_{app} in Figures 4−8 for $\Delta E^0 = E^0_{A/A^-} - E^0_{D^+/D} = 0$.

Figures 4 and 5 illustrate the V_{app} dependence of the concentrations and fluxes at two different A_2 values ($A_{1,(3)} = 10^{11}$ s^{-1})

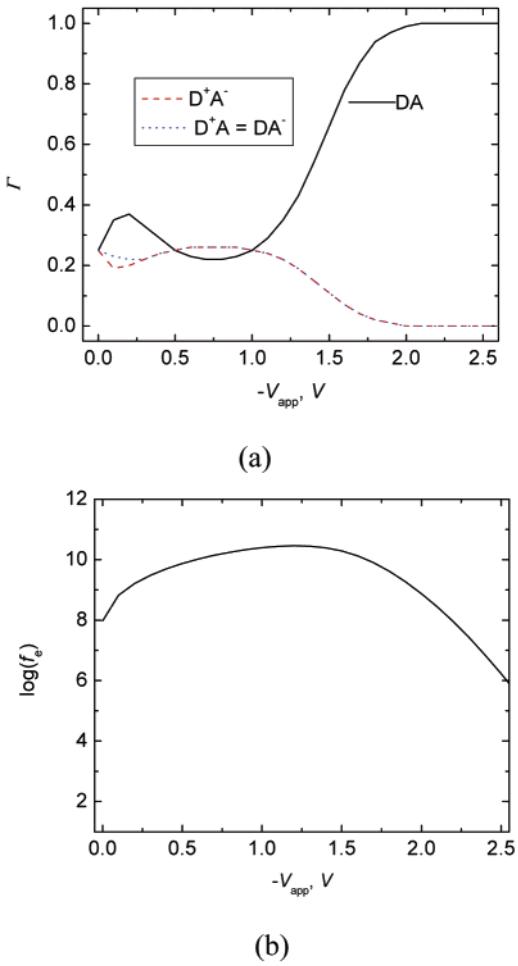

Figure 4. (a) (left) Concentrations of DA (black solid), D^+A^- (red dashed), and D^+A/DA^- (blue dotted) and (b) (right) electron flux (black solid), as a function of applied voltage with electronic factors $A_{1,3} = A_2 = 10^{11}$ s^{-1} and $\lambda_2 = 0.5$ eV, $\lambda_{1,3} = 0.25$ eV for separation distances $d_1 = d_3 = d_2/2$.

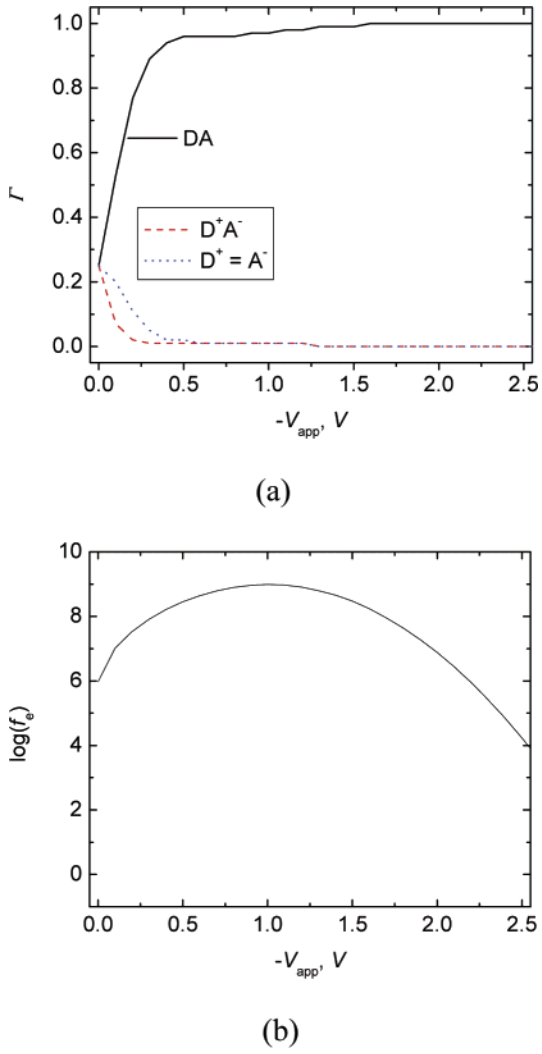

Figure 5. (a) (left) Concentrations of DA (black solid), D^+A^- (red dashed), and D^+A/DA^- and (b) (right) electron flux (black solid), as a function of applied voltage with electronic factors $A_{1,3} = 10^{11}$ s^{-1}, $A_2 = 10^9$ s^{-1} and $\lambda_2 = 0.5$ eV, $\lambda_{1,3} = 0.25$ eV for separation distances $d_1 = d_3 = d_2/2$.

for $d_1 = d_2 = 5$ Å and $d_3 = 10$ Å. Comparison of the figures shows that $\Gamma_{DA} \rightarrow \Gamma_{total}$ about 1.5 V earlier when A_2 is decreased from 10^{11} to 10^9 s^{-1}.[32] Not surprisingly, decreasing A_2 decreases the flux at a given V_{app} in the normal region, but the effect is much greater in the inverted region. Comparison of Figure 6, where $d_1 = d_2 = d_3 = 10$ Å, with Figure 4 shows the net effect of increasing $\Delta\phi_{1,(3)}/\Delta\phi_{II/I}$ from $^1/_4$ to $^1/_3$ and decreasing $\Delta\phi_2/\Delta\phi_{II/I}$ from $^1/_2$ to $^1/_3$ while maintaining $A_2 = A_{1,(3)} = 10^{11}$ s^{-1}. The result is not striking: $\Gamma_{DA} \rightarrow \Gamma_{total}$ at an applied potential about 1 V larger (more negative) and the onset of the inverted region is somewhat later. Figures 7 and 8 illustrate the dramatic effect of decreasing $A_{1,(3)}$ from 10^{12} to 10^{10} s^{-1} and increasing A_2 from 10^{10} to 10^{12} s^{-1} for $d_1 = d_2 = d_3 = 10$ Å: for $\Gamma_{DA} \rightarrow \Gamma_{total}$, the applied potential must be ~3 V greater. Furthermore, the electron flux in the normal region is relatively independent of applied voltage and the onset of the inverted region is significantly delayed.

6. Thermally Activated Hopping vs Tunneling

The above analysis has focused on a nearest-neighbor, thermally activated hopping mechanism for electron transport from electrode I to electrode II. In particular, the treatment predicts a decrease in electron flux with increasing applied voltage at large driving forces due to an increasingly unfavorable nuclear factor. However when the hopping rate becomes very small an alternative electron transport pathway involving electron (or hole) tunneling between the electrodes may become competitive.[15]

$$(e^-)I-B_1\text{-}D-B_2\text{-}A-B_3-II \rightarrow I-B_1\text{-}D-B_2\text{-}A-B_3-II(e^-) \quad (77)$$

To distinquish between the various mechanisms, we restrict the use of "tunneling" to nonthermally activated transport of an electron (or hole) from electrode I to electrode II (eq 77), whereas "hopping" is used to denote thermally activated transfer to or from a DBA site. Between the extremes of proximal (neighboring site) hopping and electrode-to-electrode tunneling is a variable range hopping mechanism that allows for hopping to distal (nonnearest neighbor) sites. An example of the latter is electron transfer from I to A in DBA (distal hopping) followed by transfer from A to II (proximal hopping)

$$(e^-)I-B_1\text{-}D-B_2\text{-}A-B_3-II \rightarrow I-B_1\text{-}D-B_2\text{-}A(e^-)\text{-}B_3-II \quad (78)$$

$$I-B_1\text{-}D-B_2\text{-}A(e^-)\text{-}B_3-II \rightarrow I-B_1\text{-}D-B_2\text{-}A-B_3-II(e^-) \quad (79)$$

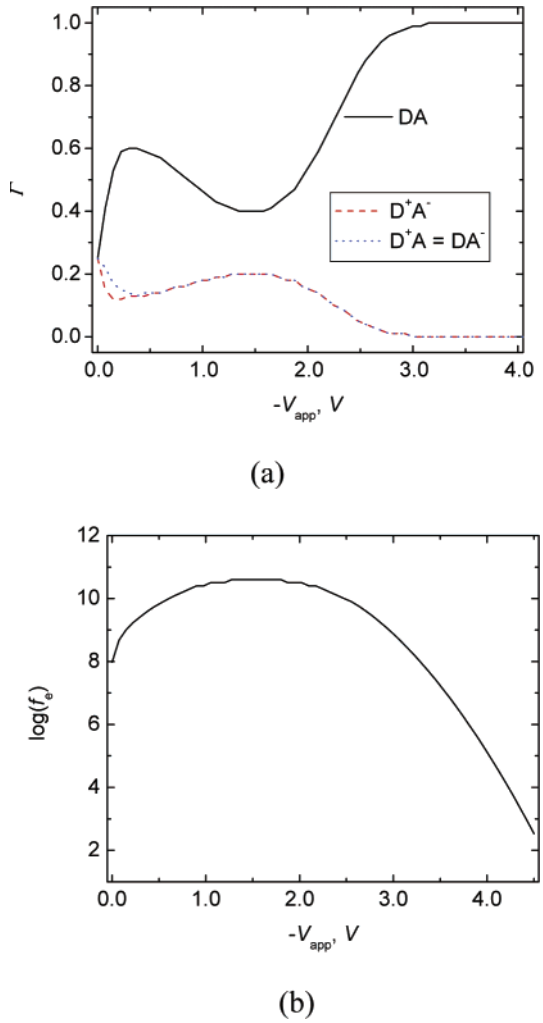

Figure 6. (a) (left) Concentrations of DA (black solid), D^+A^- (red dashed), and D^+A/DA^- and (b) (right) electron flux (black solid), as a function of applied voltage with electronic factors $A_{1,3} = A_2 = 10^{11}$ s^{-1} and $\lambda_2 = 0.5$ eV, $\lambda_{1,3} = 0.25$ eV for separation distances $d_1 = d_3 = d_2$.

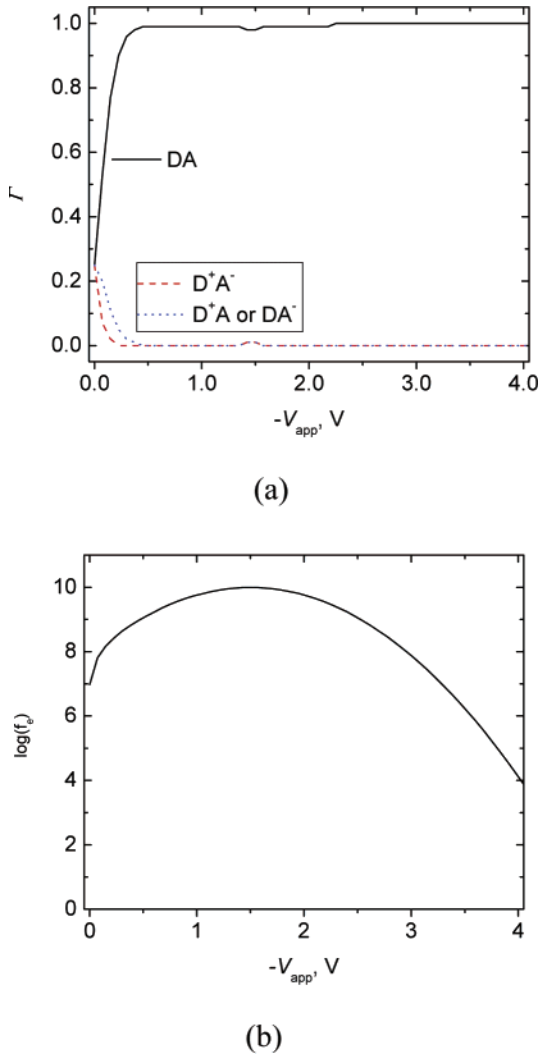

Figure 7. (a) (left) Concentrations of DA (black solid), D^+A^- (red dashed), and $D^+A/DA^-$and (b) (right) electron flux (black solid), as a function of applied voltage with electronic factors $A_{1,3} = 10^{12}$ s^{-1}, $A_2 = 10^{10}$ s^{-1} and $\lambda_2 = 0.5$ eV, $\lambda_{1,3} = 0.25$ eV for separation distances $d_1 = d_3 = d_2$.

Another example of variable range hopping is proximal hopping from I to D^+ in D^+BA^- followed by distal hopping from D to II

$$(e^-)I-B_1-D^+-B_2-A^--B_3-II \rightarrow I-B_1-D^+(e^-)-B_2-A^--B_3-II \quad (80)$$

$$I-B_1-D^+(e^-)-B_2-A^--B_3-II \rightarrow I-B_1-D^+-B_2-A^--B_3-II(e^-) \quad (81)$$

Distal transfer from D in DB_2A to II is considered less important since the transferring electron will very likely be trapped (localized) on the intervening A. Similarly, an electron transferring from I to A in D^+B_2A is likely to be trapped on the intervening D^+.[33−35]

Because of the distance dependence of the electronic coupling, a sequence of thermally activated hops generally provides the dominant mechanism for long-distance electron transport.[36,37] Another factor mitigating against efficient electron transport with the entire assembly acting as a single bridging unit is the increased probability of destructive interference of hole- and electron-transfer pathways in long bridges.[31] Nevertheless, tunneling will become more important as the hopping rate decreases in the inverted region. In contrast to hopping, the tunneling rate depends solely on the electronic interaction of the electrode sites via the intervening system and not on the nuclear factor. Thus, tunneling may provide the dominant electron transport mechanism in systems with small nuclear factors, that is, with large reorganization energies and a small driving force ($\lambda_2 \gg |\Delta\bar{G}_2^0|$) or a very large driving force ($\lambda_2 \ll |\Delta\bar{G}_2^0|$). The latter situation is of interest here.

The transition from proximal hopping to electrode-to-electrode tunneling will occur when $k_{tun}\Gamma_{total} > k_2\Gamma_{DA}$. For the present purpose, we approximate the tunneling rate constant by

$$k_{tun} = eV_{app}\left(\frac{4\pi^2}{h}\right)\rho_I\rho_{II}H_{I,II}{}^2 \quad (82)$$

which is valid in the small applied-voltage limit.[38] Within the superexchange framework, the electronic coupling element for tunneling is

$$H_{I,II} = \frac{T_{I,1(1)}t_1^{m-1}t_{1(m),2(1)}t_2^{n-1}t_{2(n),3(1)}t_3^{p-1}T_{3(p),II}}{\Delta_1^n\,\Delta_2^m\,\Delta_3^p} \quad (83)$$

where m, n, and p are the number of bridging units and t_1, t_2, and t_3 are the nearest neighbor coupling elements in B_1, B_2,

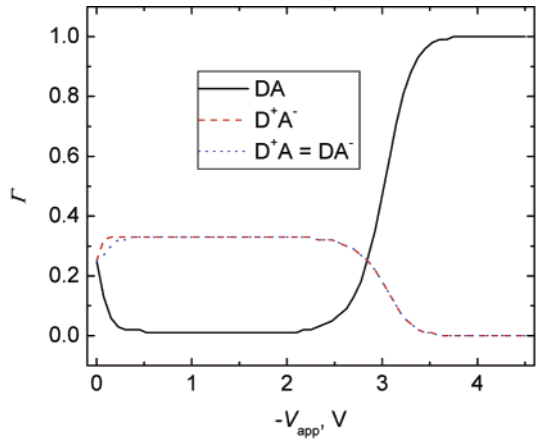

(a)

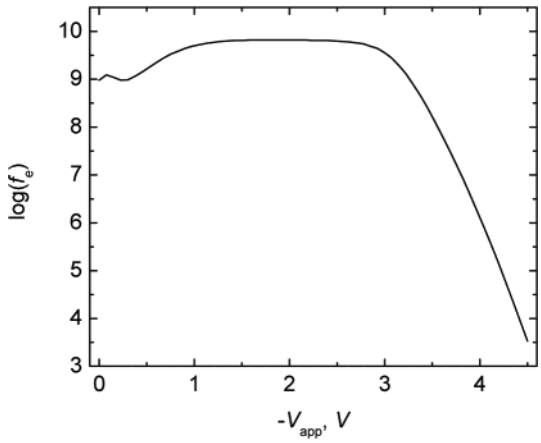

(b)

Figure 8. (a) (left) Concentrations of DA (black solid), D^+A^- (red dashed), and D^+A/DA^- (blue dotted) and (b) (right) electron flux (black solid), as a function of applied voltage with electronic factors $A_{1,3} = 10^{10}$ s^{-1}, $A_2 = 10^{12}$ s^{-1} and $\lambda_2 = 0.5$ eV, $\lambda_{1,3} = 0.25$ eV for separation distances $d_1 = d_3 = d_2$.

and B_3, respectively. If $m = n = p$, $t_1 = t_2 = t_3$, and $\Delta_1 = \Delta_2 = \Delta_3$ the expression for $H_{I,II}$ reduces to

$$H_{I,II} = \frac{T_{I,1(1)} t_{1(m),2(1)} t^{m+n+p-3} t_{2(n),3(1)} T_{3(p),II}}{\Delta^{m+n+p}} \quad (84)$$

Using the same notation

$$H_2 = \frac{T_{D,2(1)} t^{n-1} T_{2(n),A}}{\Delta^n} \quad (85)$$

so that, provided $\Gamma_{DA} \sim \Gamma_{total}$ (which is generally the limit approached in the inverted region), the condition $k_{tun}\Gamma_{total} > k_2\Gamma_{DA}$ becomes $\kappa_{n,2} < \gamma_{I,II}\exp(-\beta_{tun}\Delta d)$ where

$$\gamma_{I,II} = 2eV_{app}\rho_I\rho_{II}(\pi\lambda_2 k_B T)^{1/2}\left[\frac{T_{I,1(1)} t_{1(m),2(1)} t_{2(n),3(1)} T_{3(p),II}}{\Delta^2 T_{D,2(1)} T_{2(n),A}}\right]^2 \quad (86)$$

$$\beta_{tun} = \frac{2(m+p-2)}{\Delta d}\ln\left(\frac{\Delta}{t}\right) \quad (87)$$

$$\Delta d = (d_1 + d_3) - (d_1^0 + d_3^0) \quad (88)$$

For typical systems, $\gamma_{I,II}$ will be of the order of 10^{-2}. Thus, for $\beta_{tun} = 0.6$ Å^{-1} and $\Delta d = 16$ Å, the transition from hopping to tunneling is not reached until the D to A hopping rate has decreased by a factor 10^6.[39]

Analogous considerations indicate that distal hopping from I to A will become the dominant mechanism when $\kappa_{n,2} < \gamma_{I,A}\exp[-\beta_{tun}(d_1 - d_1^0)]$ which corresponds to a reduction in the D to A hopping rate by a factor of 10^3. Similar considerations apply to other distal hopping mechanisms. Increasing d_1 and d_3 at constant d to postpone the transition to tunneling will delay the onset of the inverted region, necessitating the use of higher V_{app}. Rather than adjusting d, it may be preferable to extend the inverted region by increasing β for distal hopping (and tunneling) relative to β for adjacent hopping.

The crossover from electron (LUMO) to hole (HOMO) conduction mentioned earlier would serve to increase the distance dependence for tunneling and distal hopping. Furthermore, changes in orbital symmetry at D and A could effectively disrupt a long-range superexchange pathway. For example, if D and A are metal complexes, tunneling through D and A could involve crossover from π-bonded ligands for B_2 to σ-bonded bridging ligands for B_1 and B_3, with potential reduction in the electronic coupling elements $t_{1(m),2(1)}$ and $t_{2(n),3(1)}$ for tunneling and distal hopping. Another consideration is that the superexchange coupling in thermally activated hopping occurs at the nuclear configuration of the transition state, whereas the superexchange coupling in electrode-to-electrode tunneling occurs at the equilibrium nuclear configurations of the intervening sites. As a consequence, the energy gaps for the superexchange mixing will tend be smaller for hopping than for tunneling. Stereoelectronic restrictions could also be less severe at the transition state configuration than at the equilibrium configuration, further favoring a hopping mechanism.

7. Conclusions

The above considerations of the distance dependence and stereoelectronic effects have shown that tunneling and distal hopping are unlikely to become competitive until the rate decreases in the inverted region have become relatively large. In a complete description, hopping to sites on the bridging groups also needs to be considered. However, as long as the transport involves electron localization on two or more D, A, or bridge sites, the inverted effect should still become manifest when increasing V_{app}. The changes in free-energy profile (nuclear factor) for an electron transfer reaction that accompany a change in driving force are familiar. For a single electron transfer process such as the D to A electron transfer, rate is a function of driving force, with the rate being scaled uniformly by the electronic factor. However, for the coupled electron-transfer sequence considered here, changing electronic factors result in dramatic shifts of the reaction profile. Evidently, the combined effects of electronic factor and driving force changes on the flux in the coupled electron-transfer systems can be profound.

Acknowledgment. This research was carried out at Brookhaven National Laboratory under contract DE-AC02-98CH10886 with the U.S. Department of Energy and supported by its Division of Chemical Sciences, Office of Basic Energy Sciences.

Note Added after ASAP Posting. A variable in eq 58 was changed from that which was originally published on 7/16/2004. The correct version was posted on 7/28/2004.

References and Notes

(1) Aviram, A.; Ratner, M. A. *Chem. Phys. Lett.* **1974**, *29*, 277−283.

(2) Ratner, M. A.; Davis, B.; Kemp, M.; Mujica, V.; Roitberg, A.; Yaliraki, S. *Ann. N.Y. Acad. Sci.* **1998**, *852*, 22−37.

(3) Ratner, M. A.; Jortner, J. In *Molecular Electronics*; Ratner, M. A., Jortner, J., Eds.; Blackwell: Oxford, U.K., 1997; pp 5−72 and references therein.

(4) Nitzan, A.; Ratner, M. A. *Science* **2003**, *300*, 1384−1389.

(5) Chabinyc, M. L.; Chen, X.; Holmlin, R. E.; Jacobs, H.; Skulason, H.; Frisbie, C. D.; Mujica, V.; Ratner, M. A.; Rampi, M. A.; Whitesides, G. M. *J. Am. Chem. Soc.* **2002**, *124*, 11730−11736.

(6) Holmlin, R. E.; Haag, R.; Chabinyc, M. L.; Ismagilov, R. F.; Cohen, A. E.; Terfort, A.; Rampi, M. A.; Whitesides, G. M. *J. Am. Chem. Soc.* **2001**, *123*, 5075−5085.

(7) Reed, M. A.; Zhou, C.; Muller, C. J.; Burgin, T. P.; Tour, J. M. *Science* **1997**, *278*, 252−254.

(8) Tian, W.; Datta, S.; Hong, S.; Reifenberger, R.; Henderson, J. I.; Kubiak, C. P. *J. Chem. Phys.* **1998**, *109*, 2874−2882.

(9) Marcus, R. A.; Sutin, N. *Biochim. Biophys. Acta* **1985**, *811*, 265−322.

(10) Adams, D.; Brus, L.; Chidsey, C. E. D.; Creager, S.; Creutz, C.; Kagan, C. R.; Kamat, P. V.; Lieberman, M.; Lindsay, S.; Marcus, R. A.; Metzger, R. M.; Michel-Beyerle, M. E.; Miller, J. R.; Newton, M. D.; Rolison, D. R.; Sankey, O.; Schanze, K. S.; Yardley, J.; Zhu, X. *J. Phys. Chem. B* **2003**, *107*, 6668−6697.

(11) Sutin, N.; Brunschwig, B. S.; Creutz, C. *J. Phys. Chem B* **2003**, *107*, 10687−10690.

(12) Schmickler, W. *Chem. Phys.* **2003**, *289*, 349−357.

(13) Schmickler, W.; Rampi, M. A.; Tran, E.; Whitesides, G. M. *Faraday Discuss.* **2004**, *125*, 171−177.

(14) Experiments with assemblies such as those modeled here have been described recently in ref 13. Although the experimental details are yet to be presented, the results reported appear to be confined to observation of Nernstian, equilibrium currents.

(15) Segal, D.; Nitzan, A.; Davis, W. B.; Wasielewski, M. R.; Ratner, M. A. *J. Phys. Chem. B* **2000**, *104*, 3817−3829.

(16) Segal, D.; Nitzan, A.; Ratner, M.; Davis, W. B. *J. Phys. Chem. B* **2000**, *104*, 2790−2793.

(17) Mujica, V.; Nitzan, A.; Datta, S.; Ratner, M. A.; Kubiak, C. P. *J. Phys. Chem. B* **2003**, *107*, 91−95.

(18) Brown, T. M.; Friend, R. H.; Millard, I. S.; Lacey, D. J.; Butler, T.; Burroughes, J. H.; Cacialli, F. *J. App. Phys.* **2003**, *93*, 6159−6172.

(19) We note that similarity of this circuit to that used in the Kelvin probe. See Janata, J.; Josowicz, M. *Anal. Chem.* **1997**, *69*, A293−A296.

(20) The sign convention used here for V_{app} is opposite to that used in ref 11.

(21) Trasatti, S. *Pure Appl. Chem.* **1986**, *58*, 955−966.

(22) Our convention for rate constants is that reactions in the counterclockwise direction (left to right as written) have a positive subscript; reactions in the counterclockwise direction (right to left as written) have a negative subscript.

(23) For our present purposes, this simplification is acceptable. Furthermore, this analysis provides a template for a more detailed treatment.

(24) Marcus, R. A. *J. Chem. Phys.* **1965**, *43*, 679−701.

(25) Gosavi, S.; Marcus, R. A. *J. Phys. Chem. B* **2000**, *104*, 2067−2072.

(26) Feldberg, S. W.; Newton, M. D.; Smalley, J. F. In *Electroanalytical Chemistry Series*; Bard, A. J., Rubinstein, I., Eds.; Marcel Dekker: New York, in press.

(27) Marcus, R. A. *J. Phys. Chem.* **1963**, *67*, 853−857.

(28) Hush, N. S. *Electrochim. Acta* **1968**, *13*, 1005−1023.

(29) Newton, M. D. *Chem. Rev.* **1991**, *91*, 767−792.

(30) Smalley, J. F.; Finklea, H. O.; Chidsey, C. E. D.; Linford, M. R.; Creager, S. E.; Ferraris, J. P.; Chalfant, K.; Zawodzinsk, T.; Feldberg, S. W.; Newton, M. D. *J. Am. Chem. Soc.* **2003**, *125*, 2004−2013.

(31) Newton, M. D.; Cave, R. J. In *Molecular Electronics*; Ratner, M. A., Jortner, J., Eds.; Blackwell: Oxford, U.K., 1997; pp 73−118.

(32) Since the individual bridges are homogeneous, eq 75 can be used for the distance dependence of the coupling element; that is, β_2 is increased by 0.7 $Å^{-1}$ with $d_0 = 3$ Å.

(33) Sumi, H.; Kakitani, T. *Chem. Phys. Lett.* **1996**, *252*, 85−93.

(34) Sumi, H.; Kakitani, T. *J. Phys. Chem. B* **2001**, *105*, 9603−9622.

(35) It has been argued in refs 33 and 34 that thermally activated hopping to and from an intermediate site and tunneling through that site should be treated not as parallel processes but rather as limiting forms of a single process. A useful parameter describing the behavior of the system between these limits is the ratio of τ_{el}, the lifetime of the electron at the intermediate site, to τ_n, the nuclear reorganization (thermalization) time of the site. Trapping occurs when the structural fluctuations at the intermediate site are very rapid, whereas the tunneling limit is reached when thermalization of the site is very slow. "Hot" hopping from the intermediate before it has thermalized is the dominant mechanism between these extremes.

(36) Bixon, M.; Jortner, J. *Chem. Phys.* **2002**, *281*, 393−408.

(37) Renger, T.; Marcus, R. A. *J. Phys. Chem. A* **2003**, *107*, 8404−8419.

(38) Mujica, V.; Kemp, M.; Ratner, M. A. *J. Chem. Phys.* **1994**, *101*, 6849−6855.

(39) Note that k_{tun} and k_{lim} for the electrode reactions may decrease at high overvoltage since increasing the magnitude of the applied voltage may increase the energy gaps for the operative superexchange mechanism and hence decrease $H_{I,II}$, H_1, or H_3. However, this effect is mitigated by the decreased energy gaps for complementary superexchange mechanisms; as the energy gap for electron superexchange increases, that for hole superexchange decreases, and vice versa.